



Efficient preparation of monodisperse CaCO₃ nanoparticles as overbased nanodetergents in a high-gravity rotating packed bed reactor

Fang Kang^{a,b}, Dan Wang^b, Yuan Pu^c, Xiao-Fei Zeng^{b,*}, Jie-Xin Wang^{a,b,c,*}, Jian-Feng Chen^{a,b,c}

^a Beijing Advanced Innovation Center for Soft Matter Science and Engineering, Beijing University of Chemical Technology, Beijing 100029, PR China

^b State Key Laboratory of Organic-Inorganic Composites, Beijing University of Chemical Technology, Beijing 100029, PR China

^c Research Center of the Ministry of Education for High Gravity Engineering and Technology, Beijing University of Chemical Technology, Beijing 100029, PR China

ARTICLE INFO

Article history:

Received 27 July 2017

Received in revised form 4 November 2017

Accepted 11 November 2017

Available online 14 November 2017

Keywords:

Nanodetergents

High-gravity rotating packed bed

Monodisperse

CaCO₃ nanoparticles

Intensified gas-liquid mass transfer

ABSTRACT

The preparation of oil-soluble metal carbonate colloids is of interest in the area of lubricant additives. This study presents a novel mass-transfer intensified approach for efficient preparation of monodisperse CaCO₃ nanoparticles as overbased nanodetergents based on W/O microemulsion using a high-gravity rotating packed bed (RPB) reactor. The effects of high gravity level, gas-liquid ratio, gas and liquid flow rates were systematically investigated. The as-prepared products had good transparency, an average particle size of about 6 nm, a high storage stability of over 18 months, a solid content of 38.5 wt% and a highest total base number (TBN) of 417 mgKOH/g. As compared to conventional stirring tank reactor (STR), the product prepared in the RPB reactor had better monodispersity and stability, smaller average particle size, narrower size distribution and higher TBN. Furthermore, the RPB reactor had a greatly shortened carbonation reaction time from 120 min of STR to 53 min, increasing the production efficiency by about 56%.

© 2017 Elsevier B.V. All rights reserved.

1. Introduction

Modern machines need lubricants to extend their time of usage. Overbased detergents are very important additives in lubricant formulations, typically composing of inorganic cores stabilized by oil-soluble surfactants and lubricating base oil [1–3]. They are essentially oil-soluble colloidal nanoparticles of metal carbonate (and metal hydroxide) as an alkaline reserve to effectively neutralize both inorganic and organic acids produced during combustion, thus preventing engine corrosion and maintain cleanliness [3–5]. The detergent with calcium carbonate (CaCO₃) as the core is the most commonly used.

The total base number (TBN, the amount of mg KOH equivalent to 1 g of the substance, mgKOH/g) is one of the most important parameters for identifying detergents [6]. According to the TBN, detergents can be mainly classified into three types: medium-alkali detergent of 100–280 mgKOH/g, high-alkali detergent of 280–400 mgKOH/g and excessively overbased detergent of >400 mgKOH/g. The TBN mainly depends on the content of CaCO₃ in the detergent. In addition, the size and the dispersity of CaCO₃ nanoparticles as cores are also important parameters that strongly influence the stability and the transparency of the detergent. Therefore, it is very crucial that the size of CaCO₃ particles needs

to be controlled to <20 nm, and CaCO₃ nanoparticles have a high solid content and long-term stable dispersion in base oil [7].

Presently, the industrial synthesis of CaCO₃ detergent is commonly achieved based on a W/O microemulsion process in a conventional stirred tank reactor (STR), which mainly includes neutralization and carbonation processes [8–11]. In general, both processes are performed in base oil. The neutralization process is to make calcium sulfonate as oil-soluble surfactant in situ through the reaction of the corresponding organic acid with Ca(OH)₂. The key carbonation process is to subsequently introduce CO₂ gas to this system composed of surfactant, promoter and nonpolar solvent to form colloidal CaCO₃ nanoparticles in reverse micelles. However, there are still several challenges in the whole procedure [7]. Firstly, complex multiphase W/O microemulsions including liquid-solid and gas-liquid-solid systems occurred in the neutralization and carbonation reaction processes, which leads to low controllability and efficiency of mass transfer, thereby causing low-efficiency CO₂ utilization, long preparation time and high energy consumption. Secondly, conventional non-uniform mixing results in a wide size distribution of the droplets and some as-formed CaCO₃ particles with a relatively large size. Finally, there is usually an incomplete modification of particles resulted from the complicated multiphase processes, leading to bad dispersity and unstability of CaCO₃ nanoparticles, and low final conversion efficiency. Therefore, it is significant to develop a new controllable and efficient preparation technology with high mass-transfer efficiency and uniform reaction environment for such complicated multiphase reaction systems and obtain an acceptance from the industrial viewpoint.

* Corresponding authors.

E-mail addresses: zengxf@mail.buct.edu.cn (X.-F. Zeng), wangjx@mail.buct.edu.cn (J.-X. Wang).

Rotating packed bed (RPB) can produce high gravity surrounding (tens to hundreds of g) by centrifugal force, leading to the formation of thin liquid films and tiny liquid droplets, which could significantly intensify gas-liquid mass transfer and micromixing, and achieve rapid nucleation rate and more even spatial concentration [12–15]. As a result, the precise controllability of particle size and distribution can be obtained, which is efficiently utilized to prepare many inorganic and organic nanopowders, such as CaCO_3 , ZnO, Fe_3O_4 , ZnS, $\text{Ca}_{10}(\text{PO}_4)_6(\text{OH})_2$, $\text{Al}(\text{OH})_3$, drug, etc. [16–22]. In particular, the commercial preparation of CaCO_3 nanopowder has been achieved by utilizing the RPB reactor [17]. However, little research has been done to adopt the RPB for the preparation of transparent liquid dispersions of monodisperse nanoparticles owing to higher level of difficulty than nanopowders [23]. As compared to a conventional STR, RPB has many advantages such as smaller particle size with narrower size distribution, shorter reaction time, easier industrialization, etc. Therefore, it is a very promising industrial platform for the production of nanomaterials.

In this study, a novel mass-transfer intensified approach for efficient and large-scale preparation of high-quality monodisperse CaCO_3 nanoparticles as overbased nanodetergents using the RPB reactor was presented. The effects of high gravity level, gas-liquid ratio, gas and liquid flow rates on the particle size and distribution, the dispersity, the TBN, Ca content and the residue were investigated in detail. In addition, a traditional STR was adopted for a comparison study.

2. Experimental

2.1. Materials and setup

Analytical reagent grade methanol (99.5%), ethanol (99.7%), heptane (99.9%), ammonia carbonate (40%) and ammonia (25–28%) were purchased from Sinopharm Chemical Reagent Co. Ltd. Mineral oil (white oil, a mixture of liquid hydrocarbons refined from petroleum, 150 SN) as oil phase and petroleum sulfonic acid ($\text{Ar-SO}_3\text{H}$ (Ar : aryl group), purity >66 wt%, inorganic acid <3 wt%, $M_n \approx 470$) were provided by Hangzhou Zhenghe Petroleum Chemical Co. Ltd. A gas cylinder with CO_2 (99.5%) was received from Beijing Ruyuanruquan Technology Co. Ltd. $\text{Ca}(\text{OH})_2$ (95%) and CaO (98%) powders as raw lime were beforehand treated by mechanical pulverization, respectively. Deionized water was used throughout the study.

Fig. 1 schematically presented the experimental setup for the whole preparation procedure. The rotating packed bed (RPB) reactor is a key component. The RPB reactor mainly consists of a wire-mesh packed

rotator, a fixed casing, two liquid inlets, a gas inlet and a suspension outlet. The wire meshes have a porosity of 0.9 and a surface area of $850 \text{ m}^2/\text{m}^3$. The rotator is installed inside the fixed casing and rotates at an adjustable speed. The inner diameter ($D_1 = 2r_1$), the outer diameter ($D_2 = 2r_2$) and the axial length of the rotator are 36 mm, 84 mm and 40 mm, respectively. The high gravity level (β) of the RPB is determined by the following equations. More information could be seen in our previous papers [16,17].

$$\beta = \frac{\omega^2 r}{g}, \quad r = \sqrt{\frac{r_1^2 + r_2^2}{2}}$$

2.2. Preparation of monodispersed CaCO_3 nanoparticles in the RPB reactor

A typical preparation process mainly includes four steps. Step 2 and step 3 were performed in the RPB reactor. Step 1: 400 mL of $\text{Ar-SO}_3\text{H}$ and 400 mL of ethanol were completely mixed under vigorous stirring at a room temperature. Subsequently, ammonia solution was added dropwise into the above mixture until $\text{pH} = 7.5\text{--}8$. After the reaction mixture was placed for 24 h, the solvents were removed from the supernatant by reduced pressure distillation, thereby obtaining transparent brownish-red liquid surfactant of NH_4ArSO_3 for the subsequent neutralization process.

Step 2: 24.64 g of NH_4ArSO_3 and 28 g of white oil were dissolved in two separate 100 mL of heptane, respectively. The above two solutions, 18.4 g of methanol as cosolvent, 16.8 g of $\text{Ca}(\text{OH})_2$ and 8.48 g of CaO were subsequently added into a stirring tank with a temperature jacket in sequence. The formed suspension was further stirred, and then pumped with a flow rate of 1100 mL/min through a liquid inlet (I1) into the RPB reactor with a temperature jacket at a high gravity level of 76. The suspension from the RPB outlet entered the stirring tank with a temperature control by water bath, and was cycled back to the RPB through I1. After 15 min, the temperature was then increased to 50°C . Afterwards, 6 mL of deionized water from a tank was pumped into the RPB through another liquid inlet (I2) with a rate of 1.5 mL/min. The following neutralization reaction process lasted for 40 min to generate the surfactant of $\text{Ca}(\text{ArSO}_3)_2$.

Step 3: After the neutralization process was completed, 2 g of $(\text{NH}_4)_2\text{CO}_3$ was added into the stirring tank. Afterwards, CO_2 gas was introduced into the RPB reactor through a gas inlet with a rate of 90 mL/min. The pH value and the conductivity were monitored every 5 min. The carbonation reaction process was stopped by shutting the CO_2 valve when the pH value reached 8.5. At this moment, the

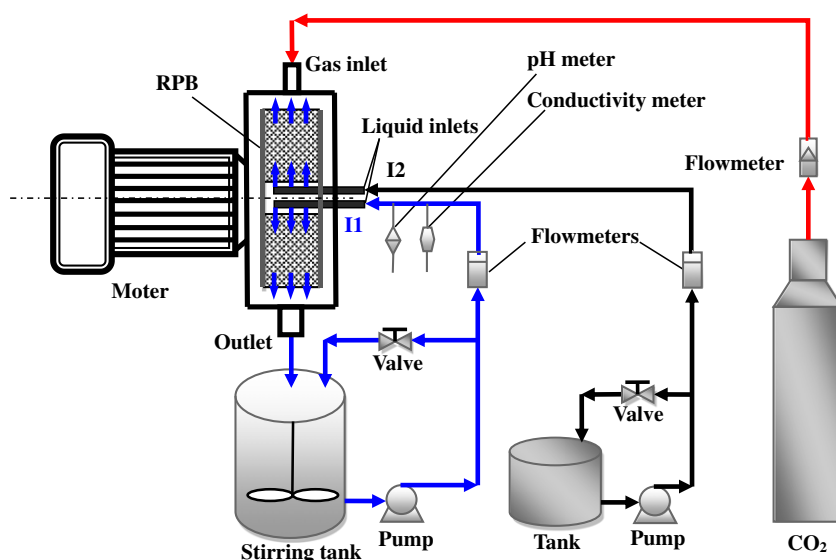


Fig. 1. Schematic diagram of experimental setup.

conductivity decreased from 0.15 to $0.10 \pm 0.02 \mu\text{S}/\text{cm}$. The introduction time of CO_2 gas usually last for 50–60 min. The RPB was stopped after 10 min.

Step 4: The residual solids were removed by centrifugation with a rotating speed of 12,000 rpm for 10 min and filtration. Heptane, methanol and water were removed by reduced pressure distillation to achieve transparent light brownish red oily liquid dispersion of monodispersed CaCO_3 nanoparticles.

For a comparison, the oil dispersion of monodispersed CaCO_3 nanoparticles was also prepared in an individual conventional stirred tank reactor (STR). The amounts and the volumes of the used materials were the same. Step 1 and 4 were performed in the same way. In step 2, 6 mL of deionized water was added into the formed mixture in the STR at 50°C controlled by water bath with a rate of 1.5 mL/min. In step 3, CO_2 gas was introduced into the STR with a rate of 90 mL/min.

2.3. Characterization

The size and the morphology of the sample were examined using transmission electron microscopy (TEM) (JEM-2010F, JEOL, Japan). The particle size distribution (PSD) was generated using image analysis and processing software (Image-Pro Plus 6.5, Media Cybernetics Inc., U.S.) according to the obtained TEM images. Thermal gravimetric (TG) analysis was performed using a thermo-gravimetric analyzer (TGS-2, PerkinElmer, USA). Fourier transform infrared (FTIR) spectrum was recorded with a Nicolet Model 6700 spectrometer (Nicolet instrument corporation) in the range of $400\text{--}4000 \text{ cm}^{-1}$. A standard potentiometric titration method according to method ASTM D2896 was used to measure the TBN. Ca content was determined by firstly burning the sample at 800°C in a muffle furnace and then dissolving it with HCl according to method ASTM D511.

3. Results and discussion

The key carbonation process was monitored by the pH value and the conductivity. Fig. 2 shows the variation of the pH value and the conductivity with the carbonation time in the RPB reactor. The conductivity had a firstly rapid decrease from 1.54 to $0.4 \mu\text{S}/\text{cm}$ in 10 min owing to a fast decrease of ion concentration from the initially preferential consumption of $(\text{NH}_4)_2\text{CO}_3$ additive and the generation of water, and then a slow reduction till $0.15 \mu\text{S}/\text{cm}$. However, the variation of the pH value had an opposite trend. There was a first relatively slow decrease from 11.5 to 10.5 in 40 min because of the initially comparative balance between the consumption and the dissolution of $\text{Ca}(\text{OH})_2$, and a subsequent quick reduction to 8.5. The carbonation reaction process was thus ended.

The rotating speed of the RPB reactor, which is the most important equipment structure parameter, can directly affect the intensified

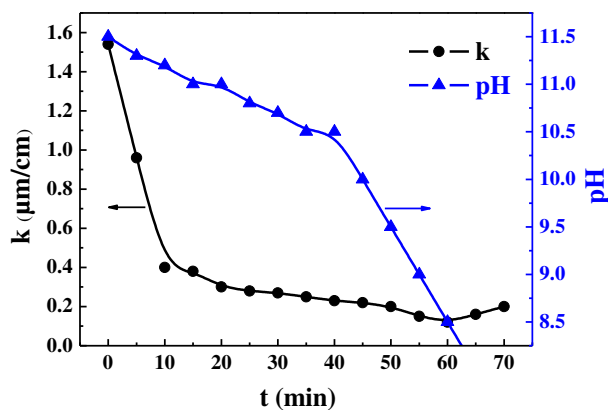


Fig. 2. The variation of the pH value and the conductivity (k) with the carbonation time in the RPB reactor.

degree of micromixing and mass transfer [14,16,17], thereby influencing the size of initial nucleation particles. Fig. 3 gives typical TEM images of oil dispersions of monodispersed CaCO_3 nanoparticles prepared at different high gravity levels and the corresponding particle size distributions. It could be clearly seen that the as-prepared CaCO_3 nanoparticles appeared monodispersed. At a low high gravity level of 21, CaCO_3 nanoparticles had an average size of 10.3 nm. With the increase of high gravity level, CaCO_3 nanoparticles became smaller and more uniform. When high gravity level reached as high as 134, CaCO_3 nanoparticles had an obviously decreased average size of 5.5 nm and a narrower size distribution. This was because the increase of high gravity level could enhance the shearing force in the RPB reactor. In this system, the fluids going through the packing were more intensively dispersed or split into thinner films, threads or tinier droplets, thereby greatly accelerating mass transfer and micromixing of fluid elements [14,20]. Moreover, mass transfer or micromixing is usually a key factor determining the supersaturation degree of the solute and its local spatial distribution in the ultra-fine particle/nanoparticle preparation based on liquid precipitation [16]. As a result, with the increase of high gravity level, the formation of supersaturation degree is rapider, more homogeneous and higher in magnitude. Accordingly, the nucleation rates at different locations become

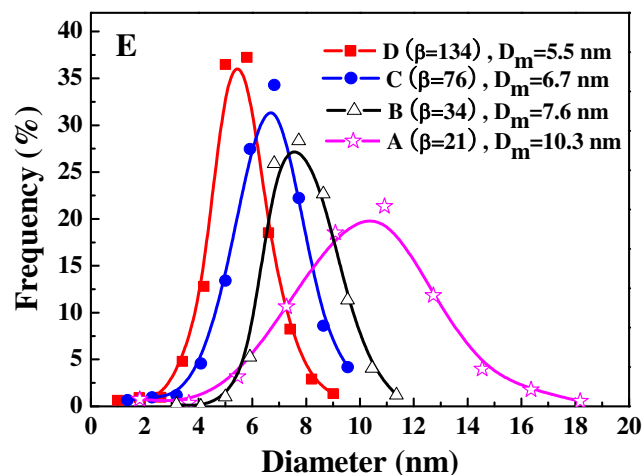
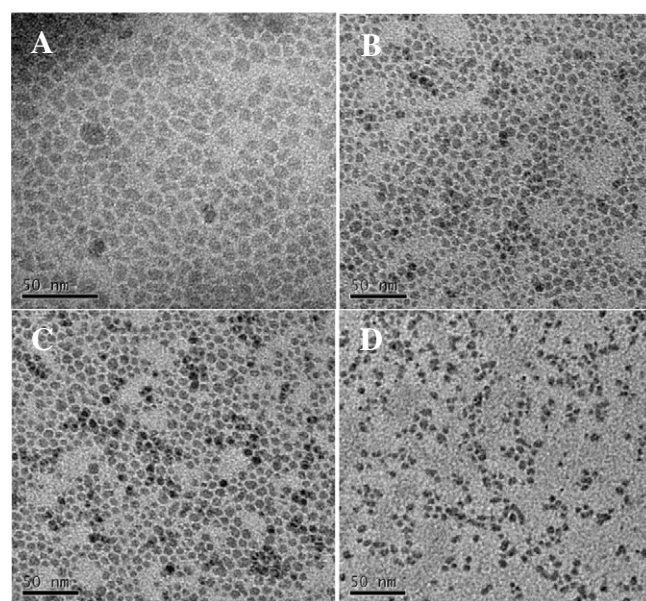


Fig. 3. TEM images of oil dispersions of monodispersed CaCO_3 nanoparticles prepared at different high gravity levels (A: 21; B: 34; C: 76; D: 134) and the corresponding particle size distributions (E) (Gas flow rate of 90 mL/min; Liquid flow rate of 1100 mL/min).

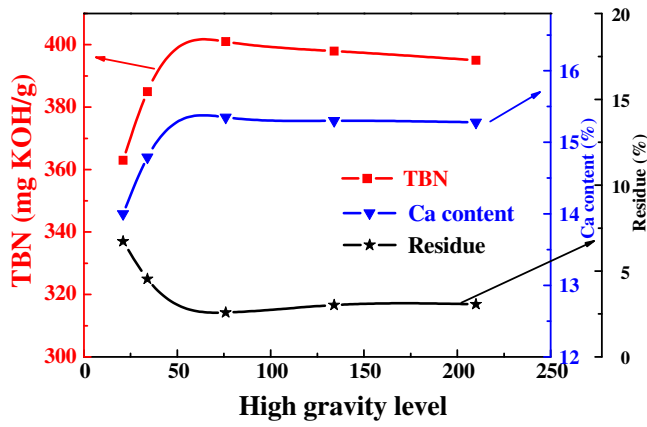


Fig. 4. Effect of high gravity level on the TBN, Ca content and the residue (Gas-liquid ratio of 0.082; Liquid flow rate of 1100 mL/min).

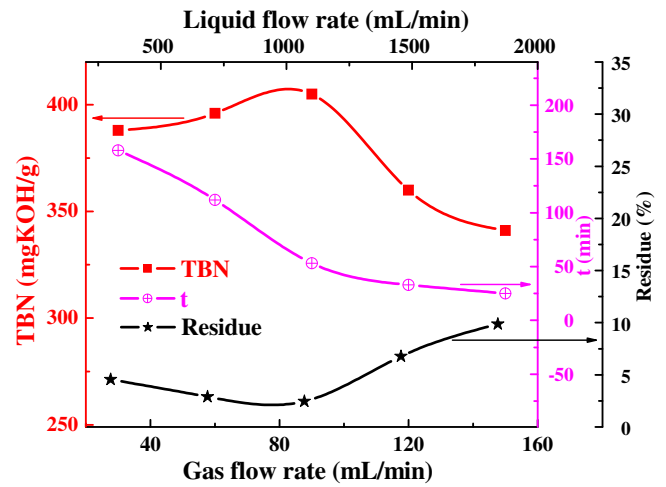


Fig. 6. Effects of gas and liquid flow rates on the TBN, the carbonation time and the residue (High gravity level of 76; Gas-liquid ratio of 0.082).

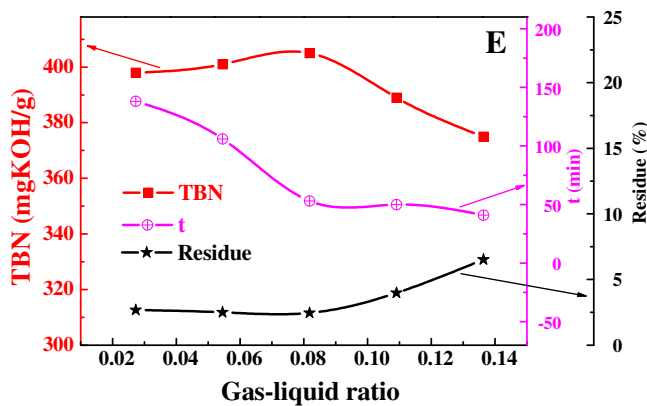
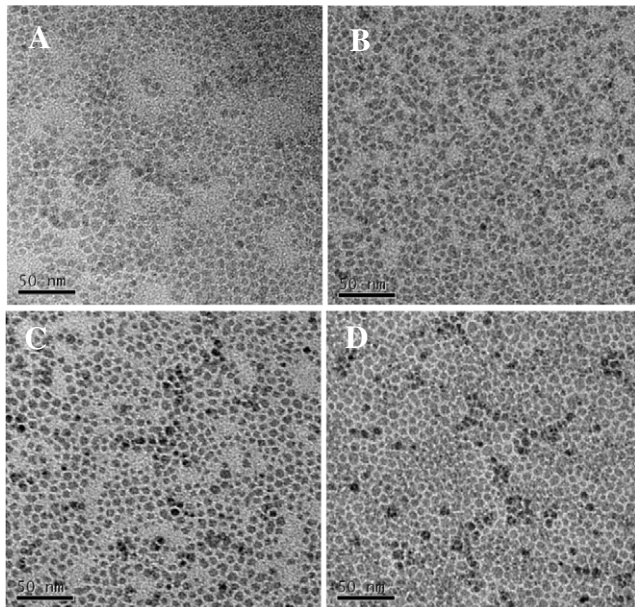


Fig. 5. TEM images of oil dispersions of monodispersed CaCO_3 nanoparticles prepared at different gas-liquid ratios (A: 0.027; B: 0.055; C: 0.082; D: 0.109), and the effect of gas-liquid ratio on the TBN, the carbonation time and the residue (E) (High gravity level of 76; Liquid flow rate of 1100 mL/min; Gas flow rate of 30 mL/min (A), 60 mL/min (B), 90 mL/min (C), 120 mL/min (D)).

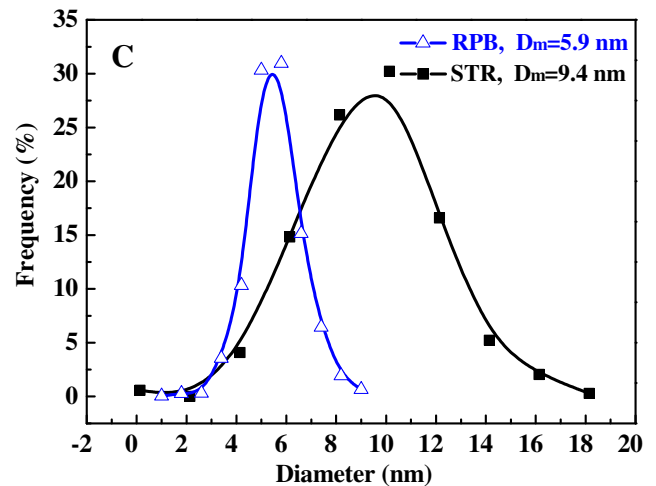
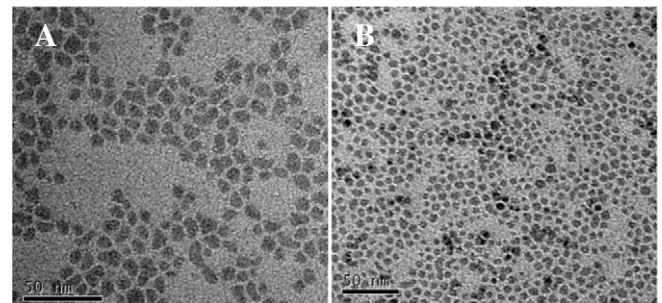


Fig. 7. TEM images of oil dispersions of monodispersed CaCO_3 nanoparticles prepared in the STR (A) and the RPB (B), and the corresponding particle size distributions (C).

mass transfer and micromixing resulted from the increase of high gravity level greatly improved the whole reaction efficiency, especially the carbonation reaction (gas-liquid mass transfer process) efficiency. $\text{Ca}(\text{OH})_2$ residue was thus obviously reduced and almost transformed to CaCO_3 nanoparticles, thereby leading to the increase of CaCO_3 content and the TBN. Therefore, a high gravity level of 76 was commonly selected in this study based on energy consumption and the quality of the product.

Fig. 5 exhibits TEM images of oil dispersions of monodispersed CaCO_3 nanoparticles prepared at different gas-liquid ratios, and the effect of gas-liquid ratio on the TBN, the carbonation time and the residue. The gas-liquid ratio is adjusted by changing the gas flow rate at a fixed liquid flow rate. It could be observed there was not an obvious difference in the particle size. By comparing four images, the product

prepared at a gas-liquid ratio of 0.082 had a relatively better monodispersity (Fig. 4C). At a gas-liquid ratio of 0.109, the oil dispersion had a higher viscosity and a worse flowability. In addition, as shown in Fig. 4E, the TBN had only a tiny increase from 398 to 405 mgKOH/g with the increase of gas-liquid ratio from 0.027 to 0.082. However, the carbonation time had a great shortening from 138 to 53 min, beneficial to the production of monodispersed CaCO_3 nanoparticles. The residue almost maintained a low level of 2.5%. Further increasing gas-liquid ratio to 0.136, the TBN had a fast decrease while the residue had an obvious increase to 6.5%. The carbonation time had only a small reduction. The possible reason is that excessive CO_2 from the overhigh gas flow rate is hard to be consumed due to a fixed liquid flow rate. Overhigh gas flow rate brings a big reduction of gas-liquid contact time, unfavorable to the carbonation reaction.

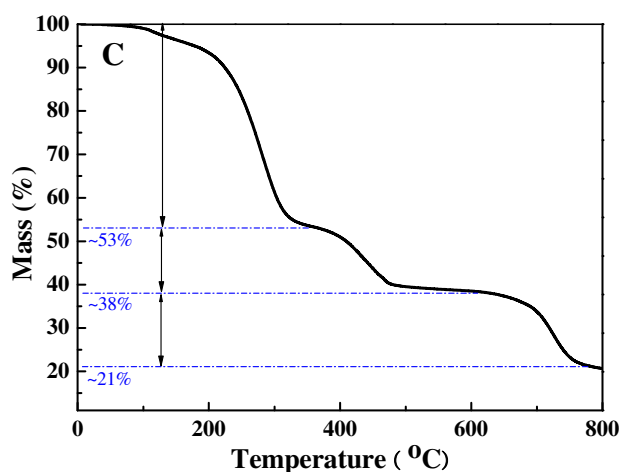
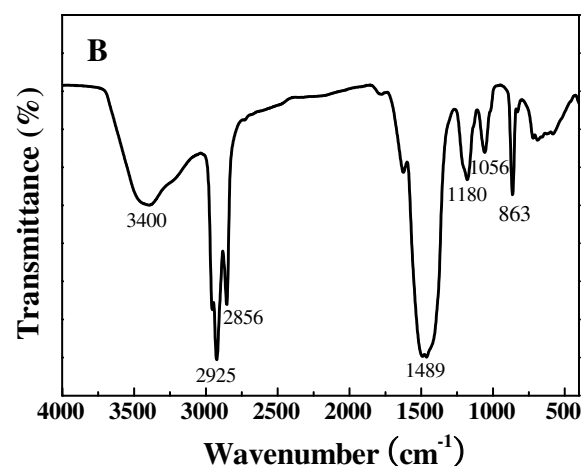
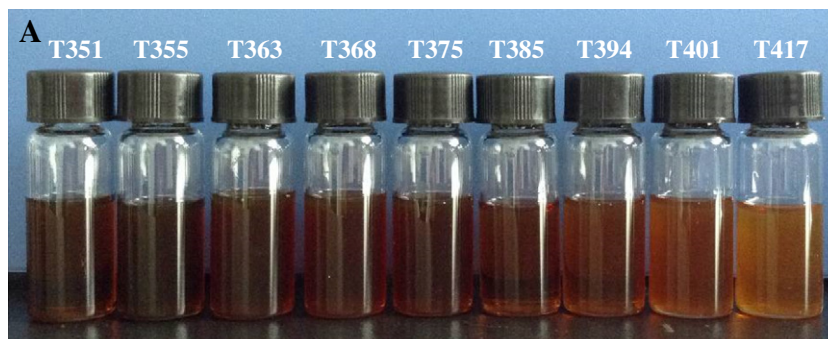


Fig. 8. Photograph (A) of oil dispersions of monodispersed CaCO_3 nanoparticles with different TBN values, FTIR spectrum (B) and TG curve (C) of oil dispersion of monodispersed CaCO_3 nanoparticles with a TBN value of 401 mgKOH/g.

Fig. 6 displays the effects of gas and liquid flow rates on the TBN, the carbonation time and the residue. At a fixed gas-liquid ratio of 0.082, the TBN firstly increased and then rapidly decreased with the increases of gas and liquid flow rates. The product had a highest TBN value of 405 mgKOH/g at a gas flow rate of 90 mL/min and a liquid flow rate of 1100 mL/min. However, the carbonation reaction time had a continuous decrease (first rapid decrease from 158 to 53 min and then a slow decrease from 53 to 25 min). Furthermore, the residue firstly slowly decreased and then rapidly increased with the increase of gas and liquid flow rates. At a gas flow rate of 90 mL/min, there was a minimum residue of 2.5%. The above phenomena could be ascribed to the fact that the increase of gas and liquid flow rates at a fixed gas liquid ratio meant more reactants and favorable gas-liquid contact. This led to the obvious acceleration of the reaction rate and the corresponding shortening of carbonation time. Extra monodispersed CaCO_3 nanoparticles were formed owing to the consumption of more reactants, facilitating the increase of the TBN and the decrease of the residue. However, too high gas and liquid flow rates would cause the formation of a larger amount of CaCO_3 particles, which were hard to timely complete phase transfer into oil phase. Some of them precipitated as the residue. Therefore, the TBN value quickly decreased from 405 to 341 mgKOH/g, while the residue obviously increased from 2.5% to 9.9%.

Fig. 7 shows TEM images of oil dispersions of monodispersed CaCO_3 nanoparticles prepared in the STR and the RPB reactor and the corresponding particle size distributions. By comparison of TEM and PSD results, it could be clearly observed that no distinct difference in the shape existed between the nanoparticles produced in both reactors. The product prepared in the STR had an average particle size of 9.4 nm and a TBN value of 397 mgKOH/g, while the product obtained in the RPB had a better monodispersity, a smaller average size of 5.9 nm, a narrower particle size distribution and a higher TBN value of 405 mgKOH/g. Furthermore, the carbonation reaction time was also greatly shortened from 120 min (STR) to 53 min (RPB), thereby improving the production efficiency by 56%. The main reason is the significantly intensified mass transfer in the RPB reactor. The mass transfer rate in the RPB is at least one to two orders of magnitude larger than that in the STR [24,25].

Fig. 8 presents a photograph of oil dispersions of monodispersed CaCO_3 nanoparticles with different TBN values prepared in the RPB, FTIR spectrum and TG curve of oil dispersion of monodispersed CaCO_3 nanoparticles with a TBN value of 401 mgKOH/g. The as-prepared oil dispersion had good transparency, a long-term storage stability over 18 months (over 12 months for STR product), and a highest TBN value of 417 mgKOH/g, belonging to excessively overbased detergent. With the increase of the TBN value, the oil dispersion appeared lighter and lighter brownish red color. This is because higher TBN means higher CaCO_3 content, and more “white color” from higher CaCO_3 content dilutes deep brownish red color. In addition, it could be found there was a sharp band at 863 cm^{-1} in FTIR spectrum, which was attributed to amorphous CaCO_3 because of the formation of colloidal CaCO_3 nanoparticles [6,26]. The strong bands at 2925 and 2856 cm^{-1} for C—H and C—C vibrations, the bands at 1180 and 1056 cm^{-1} for O = S = O vibration in sulphate belonged to the Ar- SO_3 group of the surfactant absorbed on the surface of CaCO_3 nanoparticles [7]. This indicated a high degree of CaCO_3 modification by the surfactant of $\text{Ca}(\text{ArSO}_3)_2$. Furthermore, TG result showed that the weight loss of oil dispersion was mainly divided into three stages. The first stage of weight loss was about 47% mainly ascribed to the decomposition of white oil as dispersion medium. The second stage of weight loss was about 15%, mainly resulted from the decomposition of Ar- SO_3 group of the surfactant. The final stage of weight loss was about 17% mainly owing to the decomposition of CaCO_3 to CaO, which was calculated to be Ca content of about 15.4%, almost in accordant with the result (Fig. 4) obtained using method ASTM D511. Based on the above analysis, it could be concluded that this overbased oil detergent system was composed of 38.5% amorphous CaCO_3 nanoparticles as cores modified by ~15% oil-soluble surfactant of $\text{Ca}(\text{ArSO}_3)_2$ with a surface

bonding action of $\text{Ca}(\text{ArSO}_3)_2 \cdot x\text{CaCO}_3$, and ~47% white oil as disperse medium.

4. Conclusions

In this study, a novel mass-transfer intensified approach was developed for efficient and large-scale preparation of high-quality monodispersed CaCO_3 nanoparticles as overbased oil nanodetergents by adopting a RPB reactor. The effects of high gravity level, gas-liquid ratio, gas and liquid flow rates on the particle size and distribution, the dispersity, the TBN, Ca content and the residue were explored. The results indicated that the optimal conditions of high gravity level of 76 g, gas-liquid ratio of 0.082, gas flow rate of 90 mL/min and liquid flow rate of 1100 mL/min could achieve a high utilization ratio of CO_2 and a high product yield. The as-prepared liquid-state nanodetergents were CaCO_3 nanoparticles coated with oil-soluble surfactant of $[\text{Ca}(\text{Ar}-\text{SO}_3)_2]$ monodispersed in oil, which had an average particle size of 6 nm, a high stability of >18 months, a solid content of 38.5 wt%. The TBN of the oil nanodetergent could be regulated in the range of 340–417 mgKOH/g. By comparison with the STR, it could be concluded that the product prepared in the RPB reactor had a better monodispersity, a smaller average particle size, a narrower size distribution and a higher TBN value. Furthermore, the carbonation reaction time was markedly shortened from 120 min (STR) to 53 min (RPB), improving the production efficiency by 56%. This process intensification approach based on the RPB reactor will be a promising pathway to the commercial mass production of high-quality overbased oil nanodetergents. The possible complicated formation mechanism needs to be further investigated in more detail in the future.

Acknowledgments

This work was financially supported by National Key Research and Development Program of China (2016YFA0201701/2016YFA0201700), National Natural Science Foundation of China (21622601 and 21576022) and Guangdong Provincial Applied Science and Technology Research and Development Project (2015B090927001).

References

- [1] V.N. Bakunin, A.Y. Suslov, G.N. Kuzmina, O.P. Parenago, Synthesis and application of inorganic nanoparticles as lubricant components—a review, *J. Nanopart. Res.* 6 (2004) 273–284.
- [2] L. Cizaire, J.M. Martin, T. Le Mogne, E. Gresser, Chemical analysis of overbased calcium sulfonate detergents by coupling XPS, ToF-SIMS, XANES, and EFTEM, *Colloids Surf. A Physicochem. Eng. Asp.* 238 (2004) 151–158.
- [3] A. Celik, B. Besergil, Determination of synthesis conditions of neutral calcium sulfonate, so-called detergent-dispersant, *Ind. Lubr. Tribol.* 56 (2004) 226–230.
- [4] J. Galsworthy, S. Hammond, D. Hone, Oil-soluble colloidal additives, *Curr. Opin. Colloid Interface Sci.* 5 (2000) 274–279.
- [5] L.K. Hudson, J. Eastoe, P.J. Dowling, Nanotechnology in action: overbased nanodetergents as lubricant oil additives, *Adv. Colloid Interface Sci.* 123 (2006) 425–431.
- [6] B. Besergil, A. Akin, S. Celik, Determination of synthesis conditions of medium, high, and overbased alkali calcium sulfonate, *Ind. Eng. Chem. Res.* 46 (2007) 1867–1873.
- [7] L. Du, Y.J. Wang, K. Wang, G.S. Luo, Preparation of calcium benzene sulfonate detergents by a microdispersion process, *Ind. Eng. Chem. Res.* 52 (2013) 10699–10706.
- [8] Z.C. Chen, S. Xiao, F. Chen, D.Z. Chen, J.L. Fang, M. Zhao, Calcium carbonate phase transformations during the carbonation reaction of calcium heavy alkylbenzene sulfonate overbased nanodetergents preparation, *J. Colloid Interface Sci.* 359 (2011) 56–67.
- [9] Z.C. Chen, F. Chen, D.Z. Chen, Universal phase transformation mechanism and substituted alkyl length and number effect for the preparation of overbased detergents based on calcium alkylbenzene sulfonates, *Ind. Eng. Chem. Res.* 52 (2013) 12748–12762.
- [10] T.S. Chang, H. Masood, R. Yunus, U. Rashid, T.S.Y. Choong, D.R.A. Biak, Activity of calcium methoxide catalyst for synthesis of high oleic palm oil based trimethylolpropane triesters as lubricant base stock, *Ind. Eng. Chem. Res.* 51 (2012) 5438–5442.
- [11] N. Han, L. Shui, W.M. Liu, Q.J. Xue, Y.S. Sun, Study of the lubrication mechanism of overbased Ca sulfonate on additives containing S or P, *Tribol. Lett.* 14 (2003) 269–274.

- [12] H.J. Yang, G.W. Chu, J.W. Zhang, Z.G. Shen, J.F. Chen, Micromixing efficiency in a rotating packed bed: experiments and simulation, *Ind. Eng. Chem. Res.* 44 (2005) 7730–7737.
- [13] F. Yi, H.K. Zou, G.W. Chu, L. Shao, J.F. Chen, Modeling and experimental studies on absorption of CO₂ by Benfield solution in rotating packed bed, *Chem. Eng. J.* 145 (2009) 377–384.
- [14] K. Guo, F. Guo, Y.D. Feng, J.F. Chen, C. Zheng, N.C. Gardner, Synchronous visual and RTD study on liquid flow in rotating packed-bed contactor, *Chem. Eng. Sci.* 55 (2000) 1699–1706.
- [15] K. Yang, G.W. Chu, H.K. Zou, B.C. Sun, L. Shao, J.F. Chen, Determination of the effective interfacial area in rotating packed bed, *Chem. Eng. J.* 168 (2011) 1377–1382.
- [16] J.F. Chen, Y.H. Wang, F. Guo, X.M. Wang, C. Zheng, Synthesis of nanoparticles with novel technology: high-gravity reactive precipitation, *Ind. Eng. Chem. Res.* 39 (2000) 948–954.
- [17] J.F. Chen, L. Shao, Mass production of nanoparticles by high gravity reactive precipitation technology with low cost, *China Particuology* 1 (2003) 64–69.
- [18] C.C. Lin, C.C. Lin, Feasibility of using a rotating packed bed with blade packings to produce ZnO nanoparticles, *Powder Technol.* 313 (2017) 60–67.
- [19] C.C. Lin, J.M. Ho, M.S. Wu, Continuous preparation of Fe₃O₄ nanoparticles using a rotating packed bed: dependence of size and magnetic property on temperature, *Powder Technol.* 274 (2015) 441–445.
- [20] Q. Yang, J.X. Wang, F. Guo, J.F. Chen, Preparation of hydroxyapatite nanoparticles by using high-gravity reactive precipitation combined with hydrothermal method, *Ind. Eng. Chem. Res.* 49 (2010) 9857–9863.
- [21] J.F. Chen, L. Shao, F. Guo, X.M. Wang, Synthesis of nano-fibers of aluminum hydroxide in novel rotating packed bed reactor, *Chem. Eng. Sci.* 58 (2003) 569–575.
- [22] J.F. Chen, M.Y. Zhou, L. Shao, Y.Y. Wang, J. Yun, N.Y.K. Chew, H.K. Chan, Feasibility of preparing nanodrugs by high-gravity reactive precipitation, *Int. J. Pharm.* 269 (2004) 267–274.
- [23] X.W. Han, X.F. Zeng, J. Zhang, H.F. Huan, J.X. Wang, N.R. Foster, J.F. Chen, Synthesis of transparent dispersion of monodispersed silver nanoparticles with excellent conductive performance using high-gravity technology, *Chem. Eng. J.* 296 (2016) 182–190.
- [24] Y.S. Chen, Correlations of mass transfer coefficients in a rotating packed bed, *Ind. Eng. Chem. Res.* 50 (2011) 1778–1785.
- [25] H.J. Yang, G.W. Chu, Y. Xiang, J.F. Chen, Characterization of micromixing efficiency in rotating packed beds by chemical methods, *Chem. Eng. J.* 121 (2006) 147–152.
- [26] Y.L. Wang, X. Mamat, Z.H. He, W. Eli, A novel method of quantitative carbon dioxide for synthesizing magnesium oleate (linoleate, isostearate, and sulfonate) detergents, *Ind. Eng. Chem. Res.* 50 (2011) 8376–8378.